Materials Chemistry and Physics 255 (2020) 123543

Contents lists available at ScienceDirect

Materials Chemistry and Physics

journal homepage: www.elsevier.com/locate/matchemphys

Organophilic nano-alumina for superhydrophobic epoxy coatings

Mônica O. Penna [a,e,**], Adriana A. Silva [b], Francisca F. do Rosário [e], Sergio De Souza Camargo Jr. [a,c], Bluma G. Soares [c,d,*]

[a] Universidade Federal do Rio de Janeiro, Programa de Engenharia de Nanotecnologia – PENt-COPPE, Rio de Janeiro, RJ, Brazil
[b] Universidade Federal do Rio de Janeiro/ Escola de Química, Rio de Janeiro, RJ, Brazil
[c] Universidade Federal do Rio de Janeiro, Programa de Engenharia Metalúrgica e de Materiais - PEMM-COPPE, Rio de Janeiro, Brazil
[d] Universidade Federal do Rio de Janeiro, Instituto de Macromoléculas, Rio de Janeiro, RJ, Brazil
[e] PETROBRAS – Petroleo Brasileiro S.A., Brazil

HIGHLIGHTS

- Stearic acid functionalized alumina nanoparticle with superhydrophobic characteristics.
- Simple, fast and cost effective approach for developing epoxy-based superhydrophobic coatings.
- Functionalized alumina NP as the top layer coating provides hydrophobic character to epoxy-stainless steel system.
- Hydrophobic characteristics depend upon the filler in epoxy/hardener system.

ARTICLE INFO

Keywords:
Superhydrophobic surface
Stearic acid
Nanostructured coatings
Epoxy resin
Alumina nanoparticles

ABSTRACT

Bilayer coatings with high hydrophobic characteristics were successfully prepared by depositing alumina nanoparticles functionalized with stearic acid as top layer paint onto epoxy –based bottom coatings. More stable alumina suspensions were obtained with reflux in 2-propanol than in toluene. The dispersions of functionalized alumina NP (2 wt% and 3 wt%) in 2-propanol were applied by the spray-coating method on a stainless steel substrate previously coated with two different partially cured epoxy -based coatings: DGEBA and Novolac Type II. Results show that DGEBA-based coatings with functionalized alumina NPs displayed superhydrophobic characteristics with very little interaction with water droplets, typical of the Cassie state, due to the low surface energy promoted by the functionalized alumina NPs. The alumina-modified Novolac Type II coating presented WCA in the range of 140–145°, with strong adhesion of water droplets to the surface, characteristic of the Wenzel state, which is related to the other fillers present in the commercial resin. Based on these results, it was possible to develop superhydrophobic coating by using a fast, cost effective and environmentally-friendly approach which can be scalable to relatively great surfaces, involving alumina functionalized with fatty acids and epoxy resins with controlled curing process.

1. Introduction

Superhydrophobic nanocomposites have drawn considerable attention for both fundamental research and practical applications in the last decade, due to their excellent properties, such as self-cleaning [1–3], anti-fogging [1,4], anti-icing [5], water-oil separation [6], oil purification [7], high insulating characteristics [8], anti-biofouling [9,10], anti-scaling [11–13], liquid splash [14], wear resistant [15], and anti-corrosion properties [16–18]. The high performance of superhydrophobic coatings in these applications is due to their low wettability since these surfaces present water contact angle higher than 150° [19–23]. A superhydrophobic surface can be obtained by the association of two different factors: surface roughness and low surface energy. Surface roughness is usually constituted by a hierarchical structure of micro/nanometric dimensions, and the surface energy can be decreased by regulating the chemical composition of the surface [14, 22,24]. In the last years, many synthetic methods were developed for superhydrophobic surfaces, including electro-deposition [25], phase

* Corresponding author. Universidade Federal do Rio de Janeiro, Programa de Engenharia Metalúrgica e de Materiais - PEMM-COPPE, Rio de Janeiro, Brazil.
** Corresponding author. Universidade Federal do Rio de Janeiro, Programa de Engenharia de Nanotecnologia – PENt-COPPE, Rio de Janeiro, RJ, Brazil.
E-mail addresses: mpena@petrobras.com.br (M.O. Penna), bluma@metalmat.ufrj.br (B.G. Soares).

https://doi.org/10.1016/j.matchemphys.2020.123543
Received 5 April 2020; Received in revised form 5 July 2020; Accepted 7 July 2020
Available online 2 August 2020

separation [26], drop casting [27], spray-coating [28], plasma method [12], spin-coating [29,30], sol-gel processing [31], templating [32], and lithography [33]. Nanoparticles (NPs) are also considered promising materials to prepare superhydrophobic coatings because multi-scale roughness can be easily achieved by joining the nanoscale of primary nanoparticles with the microscale roughness of nanoparticle aggregates [34,35]. Such particles are usually modified with low surface energy compounds to impart hydrophobic characteristics and better dispersion into polymeric matrices [21,22,30,36–38]. Most of these studies refer to silica nanoparticles [30,36]. Alumina nanoparticles (NP) have been also considered important materials for developing superhydrophobic surfaces due to their relatively low cost, high modulus and high thermal resistance. The incorporation of organic moiety on the alumina NP surface is considered an effective way to decrease the surface energy and improve the hydrophobic characteristics [39]. Some studies involved the hydrophobization of alumina NP by silylation using functionalized silane [6,40,41]. However, the use of long-chain fatty acids is increasing in interest because they are cost effective and environmentally friendly when compared with fluoro-compounds. In these cases, the carboxylate groups act as bidentate ligands on the surface of metal oxide nanoparticles providing effective anchorage of the fatty acid on the nanoparticle surface. Moreover, the long alkyl chains contribute for a decreasing of the surface energy of the particle. Richard et al. functionalized alumina particles with stearic acid and applied their dispersion directly on glass slides or aluminum coupons, thus obtaining superhydrophobic surfaces with contact angle as high as 156° [38]. Barron's group used highly branched carboxylic acids in alumina nanoparticles and observed contact angle of around 155° of the corresponding coating sprayed on glass slides [37,42].

Epoxy resins are considered versatile thermosetting materials with wide range of applications due to their exceptional properties, such as easy processing, high safety, excellent solvent and chemical resistance, toughness, low shrinkage on cure, mechanical and corrosion resistance, and excellent adhesion to many substrates [43]. However, they are relatively polar, thus performing high surface energy, which limits their applications as self-cleaning, anti-fouling and water-proof coatings. Therefore, the development of epoxy coatings with superhydrophobic characteristics is of great interest to combine the excellent properties of epoxy coatings with water repellence. There are two main strategies for developing superhydrophobic epoxy coatings: by dispersing fluorine-based copolymers [44] or nanoparticles [45–49] into the epoxy system before applying the coating onto a substrate (glass slide, metals, etc.) or using bilayer coating method where nanoparticle suspensions are deposited/sprayed onto a fresh epoxy-based paint [22,35,50]. The last approach is versatile because it can provide super-hydrophobicity to different painted surfaces at large scale. Some reports have successfully developed super-hydrophobic epoxy surfaces by spraying alkyl- or fluoroalkyl silane solutions [51] or hydrophobic silica suspensions [22,35] onto epoxy-based paintings. However, few reports deal with the use of alumina dispersions on epoxy painted surfaces. Wu et al. prepared bilayer coating constituted by a bottom layer of incompletely cured epoxy resin modified with glycidoxypropyl- and perfluorodecyl-based silane and a top layer containing a suspension of alumina and modified epoxy [50]. In this case, the super-hydrophobic character was achieved by a combination of the silane-modified epoxy coating together with alumina nanoparticle.

Inspired on the importance of the subject, the novelty of the present work was to adapt the hydrophobic characteristic of alumina functionalized with stearic acid with the bilayer coating approach to develop scalable and cost effective hydrophobic epoxy resin-based coatings. The great motivation was to evaluate the possibility of extending this approach to commercial epoxy paints already employed for anti-corrosive purpose. Thus, stearic acid–functionalized alumina NP dispersion was applied as the top coating of stainless steel plaques previously coated with diglycidyl ether of bisphenol A (DGEBA) or a commercial product based on epoxy Novolac-type resin combined with the room temperature curing system. This approach has not been tested before with functionalized alumina particles and commercial epoxy-based paints. According to the results presented in the following sections, the combination of stearic acid-functionalized alumina nanoparticles and the strategy of applying these particles on the incompletely cured epoxy coating resulted in outstanding hydrophobic effect mainly when epoxy resin based on diglycidyl ether of bisphenol A was employed. This technology is highly attractive from a technological point of view because with very simple steps it allows imparting superhydrophobic characteristics to commercial epoxy coatings, on large surfaces like those already employed for anti-corrosive purpose.

2. Experimental

2.1. Materials

Alumina NPs (diameter = 13 nm; specific surface area = (100 ± 15) $m^2\ g^{-1}$) (Aeroxide-Alu), stearic acid (SA), 2-propanol, toluene and ethanol were purchased from Sigma-Aldrich. Distilled water (Millipore, 15 MΩ cm) was used throughout the experimental process. Epoxy resin-based on diglycidyl ether of bisphenol A, (DGEBA) (trade name = MC-130; flash point = 255 °C; epoxy equivalent = 185–196 g eq^{-1}) from Aditya Birla Chemicals (Thailand) was dried overnight under vacuum. The curing agent for the MC-130 based on cycloaliphatic amines (ITA-MINE CA 51L) was purchased from DDChem (Italy). Tankguard Type II system, purchased from JOTUN, is composed of Novolac based epoxy resin (compound A) and polyamide as curing agent (compound B).

2.2. Modification of alumina nanoparticles

To assess the performance of different solvents, two protocols were used for the carboxylation of alumina NPs. Briefly, 2.0 g of alumina NPs were refluxed for 23 h in toluene (200 mL) or 2-propanol (200 mL) containing 5 g of stearic acid (SA), according to the procedure adapted from the work of Alexander et al. [37]. The functionalized particles were then centrifuged for 30 min, re-suspended twice in 30 mL of 2-propanol and then 30 mL of ethanol, with centrifugation steps between each dispersion to remove the unreacted carboxylic acid and dried overnight under vacuum at 80 °C. The functionalized alumina nanoparticles were named as Al-SA_{tol} and Al-SA_{prop}, when obtained by reflux under toluene or 2-propanol, respectively.

2.3. Preparation of the epoxy coatings

Stainless steel 316 (SS 316) plates with dimensions of (2.5 × 2.5 × 0.15) cm^3 were used as substrates. Both DGEBA and Novolac Type II systems were applied on stainless steel substrates using a brush and cured for 3.5 h at 40 °C in a vacuum oven, which was determined as the best time to reach good hydrophobic properties. Then, the dispersions of alumina NPs in 2-propanol (2 wt% and 3 wt%) were applied on the substrate by spray coating. The samples were left at room temperature for 4 days before testing to guarantee the total evaporation of the solvent and complete the curing process. Three replicas were made for each sample. The thickness of the alumina layers that was applied on the epoxy coatings stayed in the range of 300–400 μm.

2.4. Nanoparticles and coating characterizations

Thermogravimetric analysis (TGA) was conducted on a DSC/TGA SDT Q600 (TA Instruments, USA). The samples were run in an open aluminium crucible under continuous air flow. The heating profile was equilibrated at 50 °C and then heated at 20 °C min^{-1} with oxygen atmosphere until 100 °C and nitrogen atmosphere until 700 °C.

Fourier transform infrared (FTIR) measurements were performed with the spectroscopy Nicolet 6700 (Thermo Scientific, USA) instrument recording spectra in the 400-4000 cm^{-1} range.

Nuclear magnetic resonance analyses (NMR) (^{27}Al MAS and ^{27}Al 3QMAS) were performed on the spectrometer DD2 400 (9.40 T magnetic field) (Agilent Technologies, USA) equipped with 4.0 mm VT CP/MAS probe. Analyses were performed at room temperature (around 22 °C).

Nanoparticle size (diameter) distribution was obtained by using a Zetasizer Nano (Nano ZS) (Malvern P analytical, UK). The solutions were prepared by weighing 0.05 wt% of the nanoparticles in 2-propanol and dispersed using an ultrasonic bath for 30 min. The presented data were the average value of three measurements.

Contact angle measurements of non-functionalized and functionalized alumina nanoparticles and the epoxy-based coatings were obtained by the sessile drop method (resulting static contact angle data) using the goniometer Attention Theta (Biolin Scientific, DE). For the nanoparticle analysis, the powder was compression molded as compact disks. The deionized water drops (average volume of the drop around 4.0 μL) were deposited in three different positions of the sample surface and the water contact angle (WCA) values were determined. Each static contact angle of deionized water drop was the average of measurements from various positions on the surface.

The scanning electron microscope (SEM) analyses of the coating surfaces were performed on a Quanta 250 (FEI) (Thermo Scientific™, USA) with field emission source (FEG). Samples were previously metalized with gold/palladium on sputter coater Metalizer K575X (Emitech Quorum, USA).

Relative roughness of the coatings was determined from images obtained by SEM, on a Quanta FEG 450 – FEI microscope, with an acceleration voltage of 10 kV and magnification of 25,000. The Gwyddion software for SPM data analysis [52] was used to acquire relative roughness data from SEM images of specimens. This is an indirect method, but it is useful to compare roughness parameters, provided that the images of the investigated samples are obtained under the same conditions and subjected to the same treatments by the software. The SEM images were obtained with rather low acceleration voltage (10 kV) to ensure that the secondary electrons reflected mainly the surface topography. Diagonal roughness profiles were obtained in the treated images, and the average roughness was estimated.

3. Results and discussion

3.1. Functionalization of alumina NPs

The extent of functionalization of alumina NPs obtained in toluene and 2-propanol was estimated by TGA. Fig. 1 compares the TGA profiles of SA and as-received alumina NPs with the functionalized NPs. As-received alumina NPs did not exhibit significant mass loss below 1000 °C (Fig. 1). The functionalized alumina NPs (Al-SA$_{tol}$ and Al-SA$_{prop}$) presented mass loss at around 400 °C and 300 °C, respectively. These temperatures were significantly higher than those observed for the pure SA, indicating that the acid was successfully incorporated into the alumina NP surface. From the residue observed in the TGA curves, it was possible to estimate the degree of SA incorporation. Thus, Al-SA$_{tol}$ and Al-SA$_{prop}$ presented a degree of SA incorporation of around 14% and 22%, respectively, indicating that the use of 2-propanol during the reflux stage of alumina NP with SA was more effective. This result may be attributed to the higher polarity of 2-propanol, which improves the alumina NP dispersion and the access of the SA onto the NP surface.

The FTIR spectra of carboxylic functionalized NPs, non-functionalized alumina NPs and stearic acid are compared in Fig. 2. The bands at 2963 and 2929 cm^{-1} (peaks a and b) in the spectra of the functionalized alumina were assigned to the stretching vibrations of C–H bonds of –CH_3 and –CH_2 groups, respectively, of the stearic acid moiety. The strong band related to the C═O stretching of SA at around 1700 cm^{-1} was replaced by bands at 1600 (peak c) and 1450 cm^{-1} (peak d), which were assigned to the asymmetric and symmetric vibration of the bidentate modes of the carboxylate ligand, confirming the covalent attachment of SA onto the alumina NP surface [38]. A similar profile was also reported by Egerton et al., who analyzed the FTIR spectrum of aluminum tristearate [53]. The authors suggested that the carboxylate is bridging rather than chelating to a single aluminum ion. These bands seemed more intense on Al-SA$_{prop}$ spectrum, suggesting a better

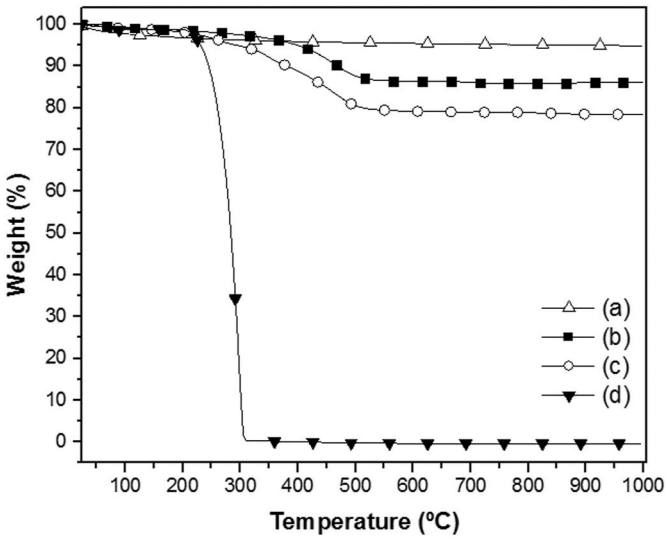

Fig. 1. TGA analysis of (a) non functionalized alumina; functionalized alumina particles: (b) Al-SA$_{tol}$ (c) Al-SA$_{prop}$ and (d) pure stearic acid.

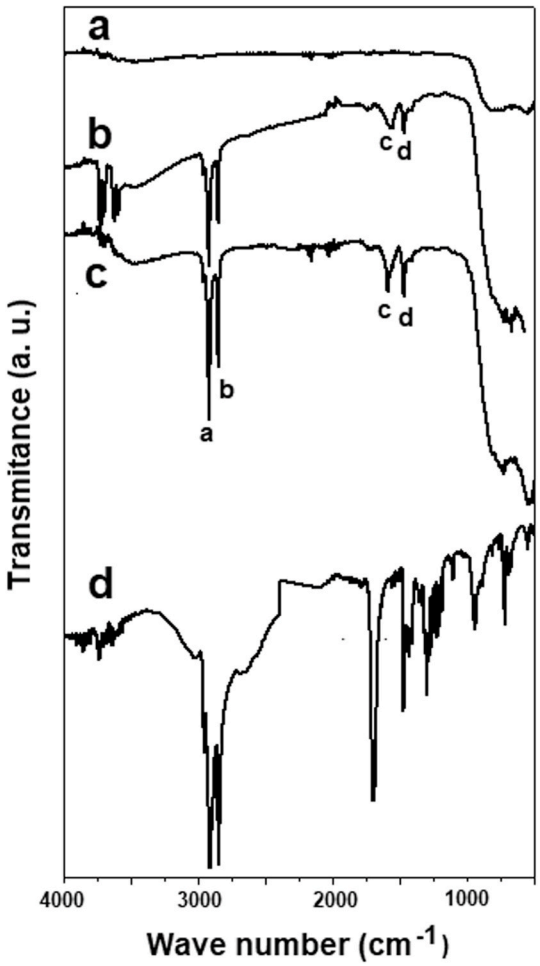

Fig. 2. FTIR spectra of (a) non functionalized alumina; functionalized alumina particles: (b) Al-SA$_{tol}$ (c) Al-SA$_{prop}$ and (d) pure stearic acid.

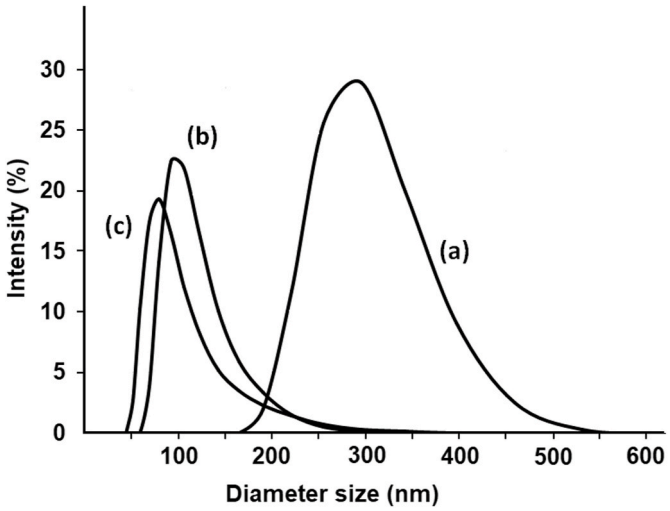

Fig. 3. Diameter size distribution of (a) non functionalized alumina; and functionalized alumina particles: Al-SA_{tol} (b) Al-SA_{prop} (c).

functionalization in case of 2-propanol reflux.

Solid-sate NMR is an important tool for characterizing several materials like alumina, zeolites, molecular sieves, polymers, nanocomposites, etc. ^{27}Al nucleus have spin number I = 5/2, known as quadrupolar nucleus. The quadrupolar interaction of such nuclei is generated from the interaction of the magnetic field with the electrical field gradient generated by the asymmetric distribution of the electrons around those nuclei. This interaction is the predominant one when observing those nuclei by NMR. So, in the 1D NMR spectra of quadrupolar nuclei (Ex: ^{27}Al MAS), the second order quadrupolar interaction is not completely cancelled, and sometimes it is difficult to distinguish species with close chemical shifts. Several experiments have been developed to eliminate the second order quadrupolar interaction. One of them is MQMAS (Multiple quantum magic angle of spinning) developed by Frydman and Harwood in 1995 [54,55]. MQMAS is a 2D pulse sequence in which in one dimension, data is collected at a multiple quantum coherence (3Q or 5Q depending on the nuclei) free from the quadrupolar interaction, so that it is possible to distinguish the isotropic chemical shifts of the resonances. In the second dimension (F2) a normal MAS spectrum is shown. The quadrupolar coupling constants of each site can be also calculated from those spectra. Although the limitation of this experiment is its low sensitivity, it has been used on a routine basis by many laboratories nowadays. Thus, the confirmation of the alumina functionalization was also possible by ^{27}Al 3QMAS (13 kHz) NMR spectra presented in Supplementary information, Fig. S1. Regarding the ^{27}Al 3QMAS spectrum obtained for the non-modified alumina nanoparticles (Fig. S1a), one can see in the F1 dimension the peaks free of the quadrupolar interaction. Therefore, by fixing the center of gravity of each resonance signals, the isotropic chemical shift can be directly read in F1. Two aluminum species can be distinguished: one small peak at ~46 ppm corresponding to a tetrahedral site (aluminum in a tetrahedral coordination) and a greater signal at ~10 ppm which is due to the presence of octahedral aluminum site (Aluminum VI). It can be noticed that the signal from the octahedral species has a gravity center but the signal spreads out in the F2 dimension. This indicates that these sites have a larger quadrupolar coupling constant when compared to those in the tetrahedral site indicating a more disordered ambient.

The ^{27}Al 3QMAS NMR spectra of the modified alumina nanoparticles displayed a new octahedral site with isotropic chemical shift around 0 ppm (F1). This site may be assigned to the Al atoms coordinated with the carboxylate groups. The results indicate that ^{27}Al 3QMAS NMR experiments contributed to confirm the attachment of the organic fatty acid chain to the alumina surface [54,55].

The effect of the functionalization on the size and size distribution of the alumina NPs was evidenced by DLS analysis performed on the dispersions in 2-propanol. Fig. 3 compares the size distributions of non-functionalized alumina NPs with those related to the SA functionalized alumina NPs prepared under reflux in toluene and 2-propanol. The average diameter of non-functionalized alumina was in the range of 293 nm. This value was significantly higher than that informed by the supplier (13 nm), indicating the presence of aggregates. The functionalization in either toluene or 2-propanol media decreased the average diameters of the alumina NPs to values in the range of 161 nm and 115 nm, respectively. Moreover, the dispersions of the functionalized alumina NPs in 2-propanol at a concentration of 0.05 wt% were stable for several weeks. This behavior suggests that the functionalization reduced the NP aggregation, thus resulting in aggregates with smaller particle sizes. The smaller average diameter of the alumina aggregates

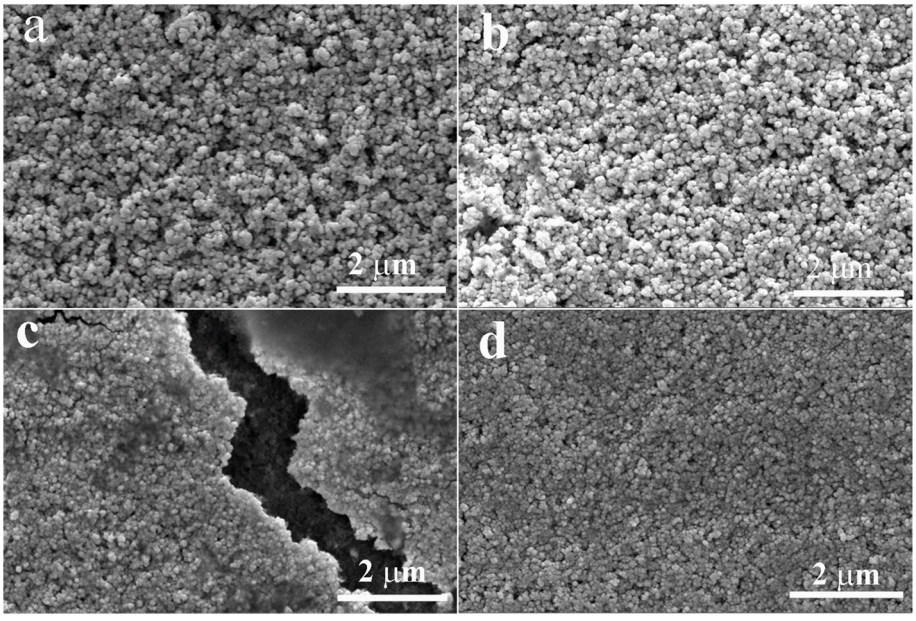

Fig. 4. SEM images of DGEBA-based epoxy coating covered with dispersion containing (a) 2 wt% and (b) 3 wt% of non-functionalized and (c) 2 wt% and (d) 3 wt% of functionalized alumina NPs.

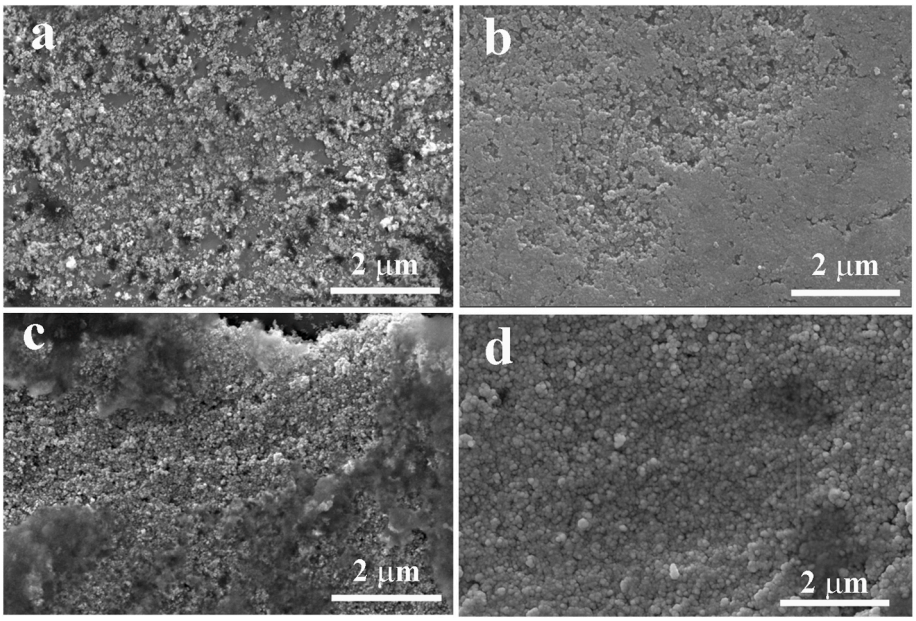

Fig. 5. SEM images of Novolac-based epoxy coating covered with dispersion containing (a) 2 wt% and (b) 3 wt% of non-functionalized and (c) 2 wt% and (d) 3 wt% of functionalized alumina NPs.

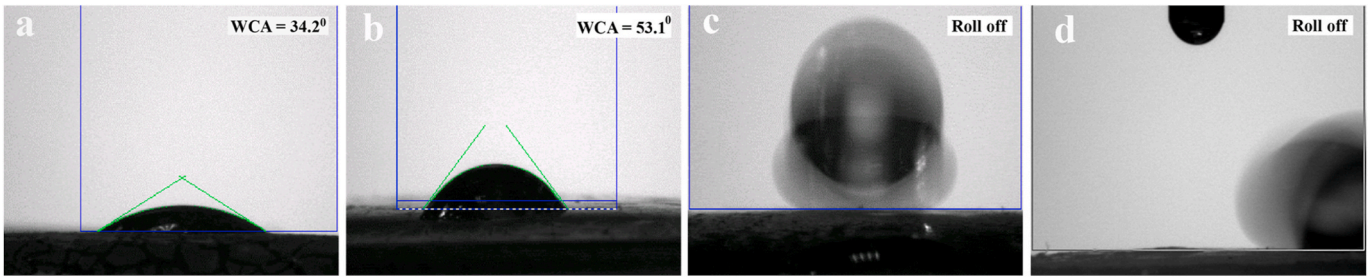

Fig. 6. Water droplet images and WCA values of DGEBA-based epoxy coating covered with dispersion containing (a) 2 wt% and (b) 3 wt% of non-functionalized and (c) 2 wt% and (d) 3 wt% of functionalized alumina NPs.

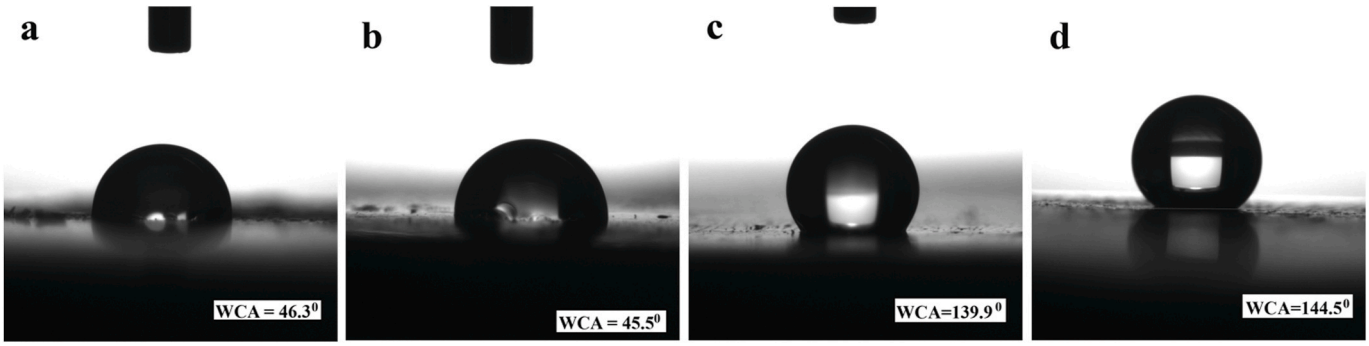

Fig. 7. Water droplet images and WCA values of Novolac-based epoxy coating covered with dispersion containing (a) 2 wt% and (b) 3 wt% of non-functionalized and (c) 2 wt% and (d) 3 wt% of functionalized alumina NPs.

functionalized in 2-propanol medium suggests, in agreement with the TGA result, the presence of higher amount of SA covering the nanoparticles, thus decreasing the chance of aggregation.

The hydrophobic character of the modified alumina NPs was evidenced by WCA measurements. The videos illustrating the water droplets on the surface of the alumina NP disks are presented in Supplementary information (Videos S1–S3). Non-functionalized alumina NP presented a hydrophilic character demonstrated by the immediate absorption of the water droplet by the corresponding surface (Video S1). On the other hand, the SA functionalized alumina NPs prepared in both toluene (Al-SA_{tol}) or 2-propanol (Al-SA_{prop}) presented a superhydrophobic character and very weak interaction with the water droplet. In the case of (Al-SA_{tol}), the water droplets remained attached to the needle even when compressed against the surface, indicating very little contact between the water and the sample surface (see Video 2). Al-SA_{prop} also displayed very low wettability, since the water droplets

Table 1
WCA and Average roughness values obtained from SEM images, for the epoxy-based coatings treated with alumina dispersions.

Alumina NP dispersion (wt. %)	Al-SA_{prop} dispersion (wt. %)	WCA (°)		Roughness (a.u.)	
		DGEBA	Novolac	DGEBA	Novolac
–	–	38 .4 ± 0.4	87.5 ± 0.5	13 × 10^{-3}	7 × 10^{-3}
2	–	34.2 ± 0.2	46.3 ± 3.1	38 × 10^{-3}	40 × 10^{-3}
3	–	53.1 ± 0.5	45.5 ± 5.2	55 × 10^{-3}	21 × 10^{-3}
–	2	Roll off	139.9 ± 4.2	34 × 10^{-3}	29 × 10^{-3}
–	3	Roll off	144.5 ± 3.4	35 × 10^{-3}	20 × 10^{-3}

immediately rolled off after touching the surface (see Video S3). Therefore, it was not possible to measure the WCA on these samples. These results are superior to those observed by Richard et al. [38] probably due to the nanosized dimension of the alumina NP used in the present work. Alexander et al. also reported water contact angles of around 155° for alumina nanoparticle functionalized with isostearic acid in toluene medium [37].

Supplementary video related to this article can be found at https://doi.org/10.1016/j.matchemphys.2020.123543

In the present paper, we demonstrated that for improved hydrophobic results it is not necessary to use fatty acids with highly branched hydrocarbon chain to functionalize the alumina NPs since cheaper stearic acid provides similar or even better effect. Moreover, our results show that reflux in 2-propanol was more effective than in toluene medium, as far as the stability and dispersion of functionalized alumina NPs are concerned. It must be added that 2-propanol also presents a great advantage from both toxicological and environmental points of view since it is less toxic than toluene. Therefore, for the preparation of the superhydrophobic coatings, functionalized alumina NPs refluxed in 2-propanol were employed.

3.2. Characterization of the superhydrophobic epoxy-based coatings

To establish the curing time of the epoxy coating for the best hydrophobic response, a dispersion containing 2.0 wt% of functionalized alumina NPs obtained in 2-propanol (Al-SA_{prop}) was sprayed on the surface of a Novolac layer cured at different times. Fig. S2 illustrates the images of WCA measurements performed on the coatings as a function of the curing time. From this Figure, it was possible to observe that the best hydrophobic character was achieved when the Novolac bottom layer was cured for 3.5 h. Lower curing times favor the embedding of the alumina NPs by the epoxy, thus decreasing the hydrophobicity and roughness. For the system cured for longer time (4.5 h), the water droplets rolled off indicating high hydrophobic character. However, the particles presented poor adhesion to the epoxy surface. Therefore, the curing protocol of 3.5 h at 40 °C in a vacuum oven was used to cure the epoxy layers.

The dispersions of alumina NPs in 2-propanol (2.0 wt% and 3.0 wt%) were applied on the stainless steel substrates previously coated with epoxy resins cured for 3.5 h at 40 °C. The SEM images of the alumina-epoxy coating surfaces are shown in Figs. 4 and 5 for DGEBA and Novolac systems, respectively. DGEBA-based coatings presented rough surfaces for both non-functionalized and functionalized alumina NPs. Nevertheless, those involving the functionalized NPs displayed slightly smaller NP size with the nanoparticles more efficiently packed, when compared with those prepared with non-functionalized NPs. By using a 3 wt% dispersion of functionalized NP, the particle distribution at the coating surface seemed to be more homogeneous (Fig. 4d).

The morphologies of the Novolac Type II-based coatings prepared with non-functionalized or functionalized alumina NPs are quite different from those observed for the DGEBA-based coatings (Fig. 5). The surface constituted by non-functionalized alumina NPs displayed a non homogeneous particle distribution on the surface, suggesting some incompatibility between the NPs and the Novolac resin. The functionalization of the NP promoted a better distribution of NPs on the surface, but it was still possible to observe some non uniform regions. These results may be attributed to the presence of several other ingredients and fillers in the commercial Novolac–based epoxy system, which may interact with the nanoparticles. According to the supplier, this commercial resin is filled with ceramic particles to provide a better reinforcing action to the coating.

The wettability of the surfaces was evaluated by static water contact angle (WCA) measurements. The WCA values of DGEBA- and Novolac-based coatings without NPs corresponded to 38.4° and 87.5°, respectively. The WCA value found for the Novolac – type coating was larger than that observed for pure DGEBA-based coating, which can be attributed to the presence of fillers in the commercial Novolac product. Figs. 6 and 7 exhibit the water droplet images and the water contact angle (WCA) values for DGEBA and Novolac systems, respectively, covered with alumina NP dispersions. The WCA values are also summarized in Table 1, together with the experimental error. For the DGEBA-based coatings, the use of non-functionalized alumina resulted in increased WCA values when 3.0 wt% of NPs was employed in the dispersion. Considering that the non functionalized alumina NP is highly hydrophilic as presented in Video 1, the slightly higher WCA for the sample prepared with the 3.0 wt% dispersion may be attributed to the surface roughness. The coating containing functionalized NPs, on the other hand, presented a very high hydrophobic character. As illustrated in Videos S4 and S5 (Supplementary Information section), these surfaces presented a very weak interaction with the water droplet, as the droplets did not adhere to the coating surface and moved back to the needle when it was removed and those that dropped down to the surface rolled off immediately. Therefore, the WCA could not be estimated. This behavior is characteristic of the Cassie state [19].

The Novolac-based coatings covered with non-functionalized NP layer resulted in a significant decrease in WCA when compared with the pure Novolac coating, indicating an increase of the hydrophilic character of these coatings. This behavior is attributed to the hydrophilic

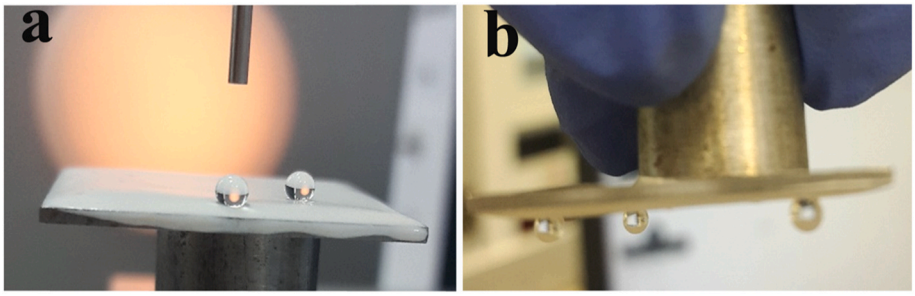

Fig. 8. Sticky property of Novolac-based epoxy coating covered with dispersion containing 3 wt% of functionalized alumina NPs.

Table 2
Water contact angle of hydrophobic surfaces containing alumina.

Coating	Substrate	WCA	Ref.
Octanoate functionalized Al_2O_3	Glass slide	143°	[42]
2-hexyldecanoate functionalized Al_2O_3	Glass slide	151°	[42]
isostearate functionalized Al_2O_3	Glass slide	154°	[37]
stearate functionalized Al_2O_3	Glass slide	156°	[38]
stearate functionalized Al_2O_3	PDMS-coated lignocellulose composite	156°	[56]
Silane funct.Al_2O_3/PDMS	Pristine fabrics	155°	[6]
isostearate funct. Al_2O_3/ epoxy resin	Plastic film	150°	[41]
Funct. Al_2O_3 with silica/ fluor-silane	Al plate etched with $CuCl_2$	164°	[41]
stearate functionalized Al_2O_3	Stainless steel coated with DGEBA epoxy resin	Roll off	This work
stearate functionalized Al_2O_3	Stainless steel coated with Novolac epoxy system	144°	This work

character of the alumina NP and the non-uniformity of the coatings observed for this surface. For the Novolac samples modified with functionalized alumina NPs, WCA values of 139.9° and 145.5° were achieved for samples prepared from dispersions containing 2.0 wt% and 3.0 wt%, respectively. Contrarily to the behavior observed for DGEBA-based coatings, the Novolac coatings containing functionalized alumina presented a strong sticky effect, where the water droplet was stuck to the alumina surface even when the surface was turned upside down as illustrated in Fig. 8. This behavior can be associated with the Wenzel-impregnating state [20], where the water droplet is partially immersed into the surface slots and may be attributed to the presence of other fillers in the Novolac composition, which promotes adhesion to the water droplets. Therefore, a balance is occurring in these coatings: the hydrophobic alumina NPs at the coating surface promote a hydrophobic effect while other fillers in the epoxy resin that may have a high affinity towards water promote a sticky effect.

Table 2 compares the WCA of different surfaces coated with alumina NPs, indicating that the approach used in the present work was successful in obtaining superhydrophobic surfaces.

Superhydrophobicity is determined by low surface energy and surface roughness. In this work, the average roughness values of the different surfaces were estimated from SEM images [57]. Fig. S4 in Supplementary information illustrates the SEM images adjusted with Gwyddion software, the 3D image of the surface, and the roughness profile of the epoxy-based coatings. Table 1 summarizes the average roughness of the samples. The surface roughness values for the epoxy-coatings containing non-functionalized and functionalized alumina NPs were higher than those of pure epoxy coatings, as expected. However, in both systems, the surfaces constituted by functionalized alumina NPs presented lower roughness values, because of the lower size of the functionalized particle aggregates, as indicated by DLS measurements. Considering the DGEBA series, when using a more concentrated dispersion (3.0 wt% of NPs) the average roughness values increased. Since the coatings prepared with functionalized NPs presented significantly higher hydrophobic character, one can conclude that the low surface energy promoted by the presence of the functionalized NPs was the main factor governing the superhydrophobic effect in these systems. In the case of Novolac-based coatings, the roughness value of the samples prepared with 2.0 wt% of non-functionalized NP dispersion was higher. However, the surface was not homogeneous, which contributed to the lower WCA values. Also in this series, the apolar nature of the functionalized NPs probably played the main role in increasing the hydrophobicity, although the presence of other fillers should contribute to diminish this effect.

4. Conclusions

Alumina nanoparticles were functionalized with stearic acid in 2-propanol and toluene refluxes and incorporated as the top layer of a bilayer epoxy-based coatings. The results showed that reflux in 2-propanol is more effective than in toluene since resulted in more stable and dispersed suspensions, due to the polar nature of 2-propanol molecules. Additionally, 2-propanol represents a great advantage over toluene since it presents less toxicological and environmental risks. The functionalized alumina NP dispersions were sprayed over partially cured epoxy-based coatings of either diglycidyl ether of bisphenol A (DGEBA) or Novolac Type II resin combined with the room temperature curing systems to produce bilayer superhydrophobic coatings.

The coatings obtained with DGEBA and functionalized alumina nanoparticles presented superhydrophobic characteristics, with very low interaction of water droplets with the surface, characteristic of the Cassie state. The analysis of WCA measurements and surface roughness values, estimated from SEM micrographs, suggests that the low surface energy promoted by the functionalized alumina NPs plays the main role in the superhydrophobic characteristics of the DGEBA/alumina system.

On the other hand, the coatings produced with Novolac Type II epoxy resin with functionalized alumina nanoparticles presented WCA values in the range of 140°–145°, with strong adhesion of water droplets to the surface, characteristic of Wenzel state, which is probably related to the nature of other fillers that are present in this commercial epoxy resin, showing that a careful choice of the epoxy matrix is crucial to obtain the desired results.

Summarizing, we have shown that superhydrophobic alumina nanoparticles can be more effectively and safely obtained in 2-propanol reflux and employed to obtain superhydrophobic nanocomposite epoxy coatings. The bilayer coating approach described in the present work involves very simple steps, is cost-effective, scalable, environmentally-friendly, and can be easily adapted to large areas. Moreover, by adjusting the coating parameters it is possible to impart superhydrophobic characteristics to commercial epoxy anti-corrosive coatings, thus enlarging its field of applications.

CRediT authorship contribution statement

Mônica O. Penna: Conceptualization, Investigation, Methodology, Writing - original draft. **Adriana A. Silva:** Investigation, Methodology, Writing - original draft. **Francisca F. do Rosário:** Conceptualization, Visualization. **Sergio De Souza Camargo:** Conceptualization, Visualization. **Bluma G. Soares:** Conceptualization, Visualization, Writing - review & editing, Supervision, Project administration.

Declaration of competing interest

The authors declare that they have no known competing financial interests or personal relationships that could have appeared to influence the work reported in this paper.

Acknowledgment

This work was sponsored in part by Conselho Nacional de Desenvolvimento Científico e Tecnológico – CNPq (Grant number 303457/2013-9), and Fundação de Amparo à Pesquisa do Estado do Rio de Janeiro – FAPERJ (Grant number E-26/202.830/2017).

Appendix A. Supplementary data

Supplementary data to this article can be found online at https://doi.org/10.1016/j.matchemphys.2020.123543.

References

[1] P. Varshney, S.S. Mohapatra, Durable and regenerable superhydrophobic coatings for brass surfaces with excellent self-cleaning and anti-fogging properties prepared by immersion technique, Tribol. Int. 123 (2018) 17–25.
[2] A. Syafiq, B. Vengadaesvaran, A.K. Pandey, N. Abd Rahim, Superhydrophilic smart coating for self-cleaning application on glass substrate, J. Nanomater. 6412601 (2018) 10.
[3] S. Liu, S.S. Latthe, H. Yang, B. Liu, R. Xing, Raspberry-like superhydrophobic silica coatings with self-cleaning properties, Ceram. Int. 41 (2015) 11719–11725.
[4] X. Gao, X. Yan, X. Yao, L. Xu, K. Zhang, J. Zhang, B. Yang, L. Jiang, The dry-style antifogging properties of mosquito compound eyes and artificial analogues prepared by soft lithography, Adv. Mater. 19 (2007) 2213–2217.
[5] S. Farhadi, M. Farzaneh, S.A. Kulinich, Anti-icing performance of superhydrophobic surfaces, Appl. Surf. Sci. 257 (14) (2011) 6264–6269.
[6] Q. J, X. Xiao, Z. Ye, N. Yu, Fabrication of durable superhydrophobic coating on fabrics surface for oil/water separation, Polym. Compos. 40 (2019) 2019–2028.
[7] N. Wang, Y. Lu, D. Xiong, C.J. Carmalt, I.P. Parkin, Designing durable and flexible superhydrophobic coatings and its application in oil purification, J. Mater. Chem. A. 4 (2016) 4107–4116.
[8] Y. Chen, D. Zhang, X. Wu, H. Wang, C. Zhang, W. Yang, Y. Chen, Epoxy/α-alumina nanocomposite with high electrical insulation performance, Prog. Nat. Sci. Mater. Int. 27 (2017) 574–581.
[9] J. Telegdi, L. Trif, L. Románszki, Smart anti-biofouling composite coatings for naval applications, Smart Compos. Coat. Membr. Transp. Struct. Environ. Energy Appl. (2015) 123–155.
[10] K.D. Sinclair, T.X. Pham, R.W. Farnsworth, D.L. Williams, C. Loc-Carrillo, L. A. Horne, S.H. Ingebretsen, R.D. Bloebaum, Development of a broad spectrum polymer-released antimicrobial coating for the prevention of resistant strain bacterial infections, J. Biomed. Mater. Res. Part A 100 (2012) 2732–2738.
[11] M.F.B. Sousa, G.F. Barbosa, F. Signorelli, C.A. Bertran, Anti-scaling properties of a SLIPS material prepared by silicon oil infusion in porous polyaniline obtained by electropolymerization, Surf. Coat. Technol. 325 (2017) 58–64.
[12] M.F.B. Sousa, C.A. Bertran, M.O. Penna, Evaluation of polymeric coatings on their efficiency of inhibiting the adhesion of inorganic scale, IOP Conf. Ser. Mater. Sci. Eng. 97 (2015), 012004.
[13] M.M. Vazirian, T.V.J. Charpentier, M.O. Penna, A. Neville, Surface inorganic scale formation in oil and gas industry: as adhesion and deposition processes, J. Pet. Sci. Eng. 137 (2016) 22–32.
[14] M. Song, J. Ju, S. Luo, Y. Han, Z. Dong, Y. Wang, Z. Gu, L. Zhang, R. Hao, L. Jiang, Controlling liquid splash on superhydrophobic surfaces by a vesicle surfactant, Sci. Adv. 3 (2017) 8, e1602188.
[15] Y. Liu, H.M. Wang, Microstructure and wear property of laser-clad Co 3 Mo 2 Si/Co ss wear resistant coatings, Surf. Coatings Technol. 205 (2010) 377–382.
[16] Y. Qing, C. Yang, C. Hu, Y. Zheng, C. Liu, A facile method to prepare superhydrophobic fluorinated polysiloxane/ZnO nanocomposite coatings with corrosion resistance, Appl. Surf. Sci. 326 (2015) 48–54.
[17] Y. Ye, D. Zhang, J. Li, T. Liu, J. Pu, H. Zho, L. Wang, One-step synthesis of superhydrophobic polyhedral oligomeric silsesquioxane-graphene oxide and its application in anti-corrosion and anti-wear fields, Corrosion Sci. 147 (2019) 9–21.
[18] E.B. Caldona, A.C.C. de Leon, B.B. Pajarito, R.C. Advincula, Novel anti-corrosion coatings from rubber-modified polybenzoxazine-based polyaniline composites, Appl. Surf. Sci. 422 (2017) 162–171.
[19] A.B.D. Cassie, S. Baxter, Wetting of porous surfaces, Trans. Faraday Soc. 40 (1944) 546–551.
[20] R.N. Wenzel, Resistance of solid surfaces to wetting by water, Ind. Eng. Chem. 28 (1936) 988–994.
[21] C. Te Hsieh, J.M. Chen, R.R. Kuo, T. Sen Lin, C.F. Wu, Influence of surface roughness on water- and oil-repellent surfaces coated with nanoparticles, Appl. Surf. Sci. 240 (2005) 318–326.
[22] M. Zhong, Y. Zhang, X. Li, X. Wu, Facile fabrication of durable superhydrophobic silica/epoxy resin coatings with compatible transparency and stability, Surf. Coat. Technol. 347 (2018) 191–198.
[23] T. Onda, S. Shibuichi, N. Satoh, K. Tsujii, Super-water-repellent fractal surfaces, Langmuir 12 (1996) 5–7.
[24] Y. Lei, Q. Wang, J. Huo, Fabrication of durable superhydrophobic coatings with hierarchical structure on inorganic radome materials, Ceram. Int. Part B 40 (2014) 10907–10914.
[25] B. Su, Y. Tian, L. Jiang, Bioinspired interfaces with super wettability: from materials to chemistry, J. Am. Chem. Soc. 138 (2016) 1727–1748.
[26] X. Ding, S. Zhou, G. Gu, L. Wu, A facile and large-area fabrication method of superhydrophobic self-cleaning fluorinated polysiloxane/TiO_2 nanocomposite coatings with long-term durability, J. Mater. Chem. 21 (2011) 6161–6164.
[27] H. Wang, F. Sun, C. Wang, Y. Zhu, H. Wang, A simple drop-casting approach to fabricate the super-hydrophobic PMMA-PSF-CNFs composite coating with heat-, wear- and corrosion-resistant properties, Colloid Polym. Sci. 294 (2016) 303–309.
[28] Z. Cui, J. Ding, L. Scoles, Q. Wang, Q. Chen, Superhydrophobic surfaces fabricated by spray-coating micelle solutions of comb copolymers, Colloid Polym. Sci. 291 (2013) 1409–1418.
[29] F. Li, M. Du, Q. Zheng, Transparent and durable SiO_2-containing superhydrophobic coatings on glass, J. Appl. Polym. Sci. 132 (2015) 41500.
[30] Z. He, M. Ma, X. Xu, J. Wang, F. Chen, H. Deng, K. Wang, Q. Zhang, Q. Fu, Fabrication of superhydrophobic coating via a facile and versatile method based on nanoparticle aggregates, Appl. Surf. Sci. 258 (2012) 2544–2550.
[31] S.S. Latthe, H. Imai, V. Ganesan, A. Venkateswara Rao, Porous superhydrophobic silica films by sol-gel process, Microporous Mesoporous Mater. 130 (2010) 115–121.
[32] Y. Wang, J. Yang, X. Guo, Q. Zhang, J. Wang, J. Ding, N. Yuan, Fabrication and tribological properties of superhydrophobic nickel films with positive and negative biomimetic microtextures, Friction 2 (2014) 287–294.
[33] A. Pozzato, S.D. Zilio, G. Fois, D. Vendramin, G. Mistura, M. Belotti, Y. Chen, M. Natali, Superhydrophobic surfaces fabricated by nanoimprint lithography, Microelectron. Eng. 83 (2006) 884–888.
[34] P. Nguyen-Tri, T.A. Nguyen, P. Carriere, C. Ngo Xuan, Nanocomposite coatings: preparation, characterization, properties, and applications, Int. J. Corros. 2018 (2018) 19. Article ID 4749501.
[35] C. Cai, N. Sang, S. Teng, Z. Shen, J. Guo, X. Zhao, Z. Guo, Superhydrophobic surface fabricated by spraying hydrophobic R974 nanoparticles and the drag reduction in water, Surf. Coat. Technol. 307 (2016) 366–373.
[36] Q. Shang, Y. Zhou, G. Xiao, A simple method for the fabrication of silica-based superhydrophobic surfaces, J. Coat. Technol. Res. 11 (2014) 509–515.
[37] S. Alexander, J. Eastoe, A.M. Lord, F. Guittard, A.R. Barron, Branched hydrocarbon low surface energy materials for superhydrophobic nanoparticle derived surfaces, ACS Appl. Mater. Interfaces 8 (2016) 660–666.
[38] E. Richard, S.T. Aruna, B.J. Basu, Superhydrophobic surfaces fabricated by surface modification of alumina particles, Appl. Surf. Sci. 258 (2012) 10199–10204.
[39] A. Llorente, B. Serrano, J. Baselga, The effect of polymer grafting in the dispersibility of alumina/polysulfone nanocomposites, Macromol. Res. 25 (2017) 11–20.
[40] G. Gu, Y. Tian, Z. Li, D. Lu, Electrostatic powder spraying process for the fabrication of stable spuperhydrophobic surfaces, Appl. Surf. Sci. 257 (2011) 4586–4588.
[41] M. Khodaei, S. Shadmani, Superhydrophobicity on aluminum through reactive-etching and TEOS/GPTMS/nano Al_2O_3 silane-based nanocomposite coating, Surf. Coat. Technol. 374 (2019) 1078–1090.
[42] W. Al-Shatty, A.M. Lord, S. Alexander, A.R. Barron, Tunable surface properties of aluminum oxide nanoparticles from highly hydrophobic to highly hydrophilic, ACS Omega 2 (2017) 2507–2514.
[43] F.L. Jin, X. Li, S.J. Park, Synthesis and application of epoxy resins: a review, J. Ind. Eng. Chem. 29 (2015) 1–11.
[44] J. Tan, W. Liu, Z. Wang, Hydrophobic epoxy resins modified by low concentration of comb-shaped fluorinated reactive modifier, Prog. Org. Coat. 105 (2017) 353–361.
[45] M. Psarki, G. Celichowski, J. Marczak, K. Gumowski, G.B. Sobieraj, Superhydrophobic dual-sized epoxy composite coatings, Surf. Coat. Technol. 225 (2013) 66–74.
[46] M. Psarki, J. Marczak, G. Celichowski, G.B. Sobieraj, K. Gumowski, F. Zhou, W. Liu, Hydrophobization of epoxy nano composite surface with 1H,1H,2H,2H-perfluor-ooctyltrichlorosilane for superhydrophobic properties, Cent. Eur. J. Phys. 10 (2012) 1197–1201.
[47] M. Psarski, D. Pawlak, J. Grobelny, G. Celichowski, Relationships between surface chemistry, nanotopography, wettability and ice adhesion in epoxy and SU-8 modified with fluoroalkylsilanes from the vapor phase, Appl. Surf. Sci. 479 (2019) 489–498.
[48] D. Hill, A.R. Barron, S. Alexander, Comparison of hydrophobicity and durability of functionalized aluminum oxide nanoparticle coatings with magnetite nanoparticles-links between morphology and wettability, J. Coll. Interface Sci. 555 (2019) 323–330.
[49] D. Pinto, A.M. Amaro, L. Bernardo, Experimental study on the surface properties of nanoalumina-filled epoxy resin nanocomposites, Appl. Sci. 10 (2020) 733.
[50] B. Wu, J. Lyu, C. Peng, D. Jiang, J. Yang, J.S. Yang, S. Xing, L. Sheng, Inverse infusion processed hierarchical structure towards superhydrophobic coatings with ultrahigh mechanical robustness, Chem. Eng. J. 387 (2020) 124066.
[51] J. Marczak, M. Kargol, M. Psarski, G. Celichowski, Modification of epoxy resin, silicon and glass surfaces with alkyl- or fluoroalkylsilanes for hydrophobic properties, Appl. Surf. Sci. 380 (2016) 91–100.
[52] D. Necas, P. Klapetek, Gwyddion: and open-source software for SPM data analysis, Cent. Eur. J. Phys. 10 (2012) 181–188.
[53] T.A. Egerton, N.J. Everall, I.R. Tooley, Characterization of TiO_2 nanoparticles surface modified with aluminum stearate, Langmuir 21 (2005) 3172–3178.
[54] L. Frydman, J.S. Harwood, Isotropic spectra of half-integer quadrupolar spins from bidimensional magic-angle spinning NMR, J. Am. Chem. Soc. 117 (1995) 5367–5368.
[55] A. Medek, J.S. Harwood, L. Frydman, Multiple-Quantum magic-angle spinning NMR: a new method for the study of quadrupolar nuclei in solids, J. Am. Chem. Soc. 117 (1995) 12779–12787.
[56] Z. Wang, X. Shen, Y. Yan, T. Qian, J. Wang, Q. Sun, C. Jin, Facile fabrication of a PDMS@ stearic acid-Al$(OH)_3$ coating on lignocellulose composite with superhydrophobicity and flame retardancy, Appl. Surf. Sci. 450 (2018) 387–395.
[57] Y. Zhang, Y. Zheng, Y. Li, L. Wang, Y. Bai, Q. Zhao, X. Xiong, Y. Cheng, Z. Tang, Y. Deng, S. Wei, Tantalum nitride-decorated titanium with enhanced resistance to microbiologically induced corrosion and mechanical property for dental application, PLoS One 10 (2015) e0130774.